

Article

# Low Gate Lag Normally-Off p-GaN/AlGaN/GaN High Electron Mobility Transistor with Zirconium Gate Metal

Chia-Hao Liu <sup>1</sup>, Hsien-Chin Chiu <sup>1,2,3,\*</sup> , Chong-Rong Huang <sup>1</sup>, Kuo-Jen Chang <sup>4</sup>, Chih-Tien Chen <sup>4</sup> and Kuang-Po Hsueh <sup>5</sup>

<sup>1</sup> Department of Electronics Engineering, Chang Gung University, Taoyuan 333, Taiwan; r3287133@gmail.com (C.-H.L.); gain525252@gmail.com (C.-R.H.)

<sup>2</sup> Department of Radiation Oncology, Chang Gung Memorial Hospital, Taoyuan 333, Taiwan

<sup>3</sup> The College of Engineering, Ming Chi University of Technology, Taishan 243, Taiwan

<sup>4</sup> Materials & Electro-Optics Research Division, National Chung-Shan Institute of Science & Technology, Longtan 325, Taiwan; mike.ckj@gmail.com (K.-J.C.); ctchen@ncsist.org.tw (C.-T.C.)

<sup>5</sup> Department of Digital Multimedia Technology, Vanung University, Chungli 32061, Taiwan; kphsueh@mail.vnu.edu.tw

\* Correspondence: hcchiu@mail.cgu.edu.tw; Tel.: +886-3-2118800-3350

Received: 15 December 2019; Accepted: 3 January 2020; Published: 6 January 2020



**Abstract:** The impact of gate metal on the leakage current and breakdown voltage of normally-off p-GaN gate high-electron-mobility-transistor (HEMT) with nickel (Ni) and zirconium (Zr) metals were studied and investigated. In this study, a Zr metal as a gate contact to p-GaN/AlGaN/GaN high mobility transistor (HEMT) was first applied to improve the hole accumulation at the high gate voltage region. In addition, the ZrN interface is also beneficial for improving the Schottky barrier with low nitrogen vacancy induced traps. The features of Zr are low work function (4.05 eV) and high melting point, which are two key parameters with p-GaN Schottky contact at reversed voltage. Therefore, Zr/p-GaN interface exhibits highly potential for GaN-based switching power device applications.

**Keywords:** normally-off; HEMT; p-GaN gate; low work function; leakage current; breakdown voltage

## 1. Introduction

Gallium nitride high-electron-mobility-transistor (HEMT) is a major candidate in the high frequency and high power device application due to the material properties, such as good thermal property, high breakdown voltage and high channel mobility. The traditional AlGaN/GaN HEMT structure is depletion-mode (D-mode) behavior [1,2]. However, two dimensional electron gas (2DEG) in traditional AlGaN/GaN HEMT structure inherently exists in the interface of GaN due to the polarization electric field in the AlGaN/GaN hetero structure.

In switching power applications with simple circuitry and fail safe requirements, normally off devices are strongly preferred. Several researches have been proposed to obtain an enhanced-mode (E-mode) HEMT, such as the fluorine treatment [3,4], a p-type GaN cap layer [1,5–8] and gate recess structure [9,10]. However, p-GaN layer will deplete the 2DEG due to the P–N junction, which achieves E-mode HEMT. The structure with p-GaN attracts tremendous attention in the industry due to its large threshold voltage, on/off ratio, as well as low on-state resistance. To further improve the performance of power device, breakdown voltage can be enhanced by the gate metal, concentration of magnesium (Mg) doping GaN, or gate dielectric. Moreover, the Schottky barrier height can be increased by the metal work function, which contacts to p-GaN [11].

The energy level of the valence band of GaN is deeper than the work function of typical metals, it performed a Schottky contact between the metal and p-GaN. The ideal Schottky barrier height ( $q\Phi_B = E_g - q(\Phi_m - \chi)$ ) can be calculated, which are 2.35 eV and 3.45 eV, respectively. To increase the Schottky barrier height, we choose the low work function metal to increase the  $\Delta E_v$ . The traditional gate metal is Ni, which the work function is 5.15 eV [12]. Moreover, based on the higher  $\Delta E_v$  consideration, the lower work function metal such as Zr was thus adopted. Moreover, the Zr was chosen in our experiment due to their low work function (4.05 eV), high melting point, and high content in nature.

The traps from surface, bulk or interface trap states can limit the performance of device. The surface traps are considered to be causes of gate lag, and the buffer traps are considered to be causes of drain lag [13]. In particular, the power device market strongly prefers E-mode structure for cost, size, safety and power consumption reasons. In this letter, we use low work function Zr to suppress hole current and increase device breakdown voltage.

## 2. Device Structure

The HEMT structure used for our devices were grown on a 6-inch p-type low resistivity Si (111) substrate by using metal organic chemical-vapor deposition (MOCVD). In Figure 1, an undoped GaN channel layer with a thickness of 300 nm was grown on buffer layer with a thickness of 4  $\mu\text{m}$ . Subsequently, a p-GaN layer, which the Mg concentration in the p-GaN layer was  $3 \times 10^{19} \text{ cm}^{-3}$  with a thickness of 70 nm were grown on an  $\text{Al}_{0.17}\text{Ga}_{0.83}\text{N}$  barrier layer with a thickness of 12 nm. The device fabricated with mesa isolation by reactive-ion etching (RIE) for the first step. Second, p-GaN layer was etched by RIE with  $\text{Cl}_2/\text{BCl}_3/\text{Ar}$ . Then, Ti/Al/Ni/Au metal film was deposited as source and drain by electron beam evaporation (E-gun) and it was annealed at 875  $^\circ\text{C}$  for 35 s in  $\text{N}_2$  atmosphere by RTA system. After all, for the comparison of high and low work function metals, Zr/Au (25/80 nm) and Ni/Au (25/80 nm) were deposited as a gate electrode by E-gun on a different device, respectively and we named the device Ni-HEMT and Zr-HEMT with the different gate. Ti/Au was deposited as the pad for interconnection. Eventually, two devices were passivated with 50 nm  $\text{Si}_3\text{N}_4$  by PECVD. By measuring the transmission-line, the ohmic contact resistance for Ni-HEMT and Zr-HEMT was  $7.1 \times 10^{-5} \Omega\cdot\text{cm}^2$  and  $7 \times 10^{-5} \Omega\cdot\text{cm}^2$ , respectively. For both the fabricated devices, the gate width was 100  $\mu\text{m}$ , gate length was 3  $\mu\text{m}$ , source–gate distance was 2  $\mu\text{m}$  and gate–drain distance was 7  $\mu\text{m}$ .

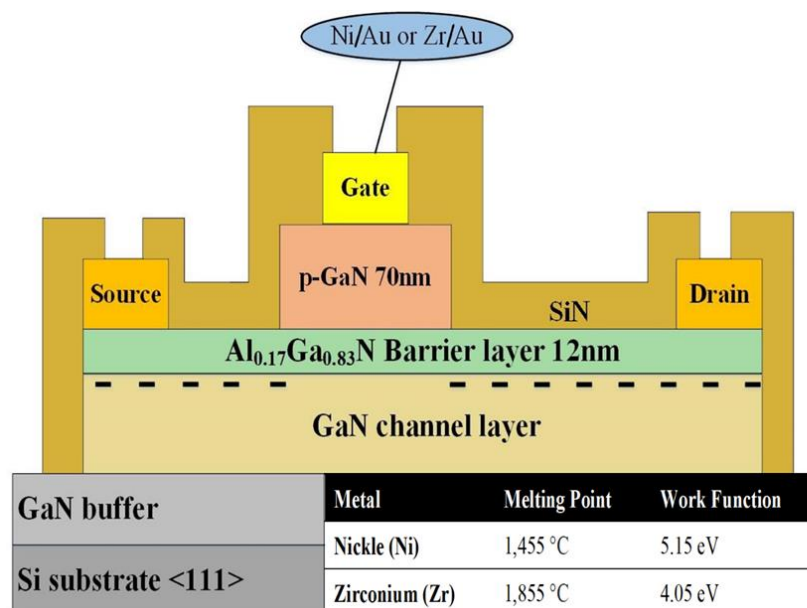


**Figure 1.** Schematic of the E-mode p-GaN/AlGaN/GaN high-electron-mobility-transistor (HEMT) with a different gate metal.

### 3. Experimental Result and Discussion

For the Zr/p-GaN interface analysis, the material composition of p-GaN gate and gate metal interface was analyzed by X-ray photoelectron spectroscopy (XPS), which was shown in Figure 2a,b. The green block is the experiment line and the black line is the fitting line. Figure 3a shows the Ni 2p<sub>3/2</sub> peaks consist of two components: Ni–Ni and Ni–O bonds, and the Figure 3b shows the Zr 3d<sub>5/2</sub> peaks consist of three components: Zr–O, Zr–N and Zr–Zr bonds. The results show that Ni was combined with O, so there is the Ni–O peak in the Ni 2p<sub>3/2</sub> peaks. However, in the Zr 3d<sub>5/2</sub> peaks, besides the Zr–O and Zr–Zr, the Zr–N peak was observed, which may improve the device performance due to the better bonding between p-GaN and Zr and ZrN is also a refractory material. By the way, the traditional nitrogen vacancies were also thus suppressed due to the formation of ZrN.

In order to study the effect of the metal/p-GaN contact on the gate leakage current and saturation current, the  $I_{DS}-V_{GS}$ ,  $I_{DS}-V_{DS}$  characteristics of Ni-HEMT and Zr-HEMT were measured. The threshold voltage ( $V_{TH}$ ) for the Zr-HEMT and Ni-HEMT was 1.5 and 1 V (defined by  $I_{DS} = 1$  mA/mm), respectively. The threshold voltage in the Zr-HEMT was higher because of the higher Schottky barrier height at the interface of p-GaN gate and metal gate compared with the Ni-HEMT. The drain ON/OFF current ratio ( $I_{ON}/I_{OFF}$ ) of the Zr-HEMT and Ni-HEMT was  $4.6 \times 10^9$  and  $8.2 \times 10^5$ , respectively, and adopting the low work function gate metal improved the subthreshold swing from 137 to 89 mV/decade. The Zr-HEMT also shows a lower drain leakage current that Zr-HEMT and Ni-HEMT were  $3 \times 10^{-8}$  mA/mm and  $1.8 \times 10^{-4}$  mA/mm, respectively, as shown in Figure 3a. The output characteristics are shown in Figure 3b. The saturated drain current of Zr-HEMT and Ni-HEMT were 141 and 169 mA/mm at  $V_{GS} = 6$  V and  $V_{DS} = 10$  V, respectively. The ON-resistance ( $R_{on}$ ) for the Zr-HEMT and Ni-HEMT at  $V_{GS} = 6$  V was 8.2 and 13  $\Omega$ -mm, respectively, which corresponds to a specific ON-resistance ( $R_{sp}$ ) of 3.08 and 2.39  $m\Omega$ -cm<sup>2</sup> at  $V_{DS} = 10$  V.

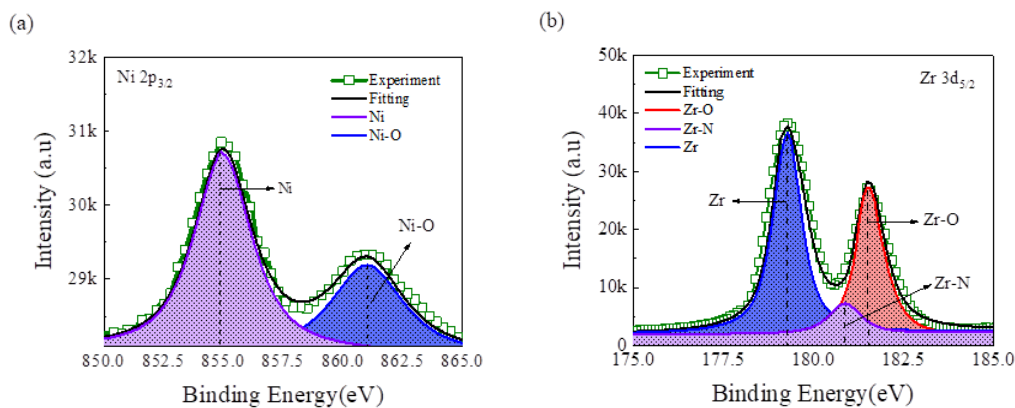


**Figure 2.** Show the X-ray photoelectron spectroscopy (XPS) spectra of (a) Ni 2p<sub>3/2</sub> and (b) of Zr 3d<sub>5/2</sub>.

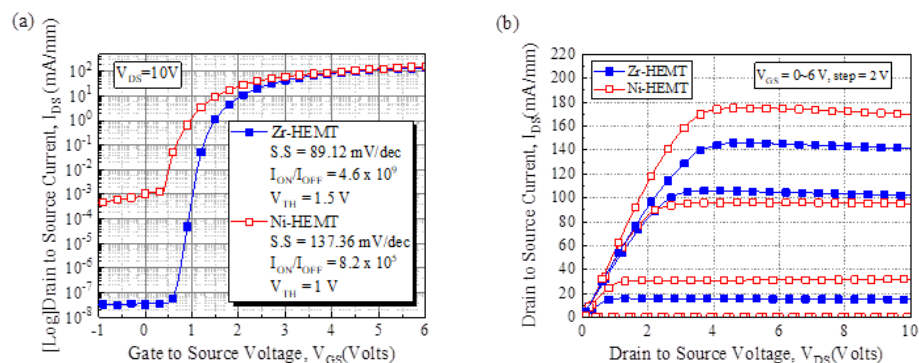


**Figure 3.** (a) Log-scale  $I_{DS}-V_{GS}$  transfer and (b)  $I_{DS}-V_{DS}$  output characteristics of the Zr-HEMT and Ni-HEMT.

In this letter, the valence band of Zr and Ni contact to p-GaN were simulated at off-state, which  $V_{GS} = -2$  V and  $V_{DS} = 100$  V by TCAD in Figure 4a,b. The low work function metal Zr contact to p-GaN will pull down valence band much lower than Ni that this phenomenon will cause higher hole accumulation. Furthermore, holes accumulation also leads to a wider depletion region effectively [12]. Therefore, Zr-gate on p-GaN can achieve comparatively high hole concentration thus improve the hole trapping phenomenon at the gate metal/p-GaN interface during fast switching behavior.

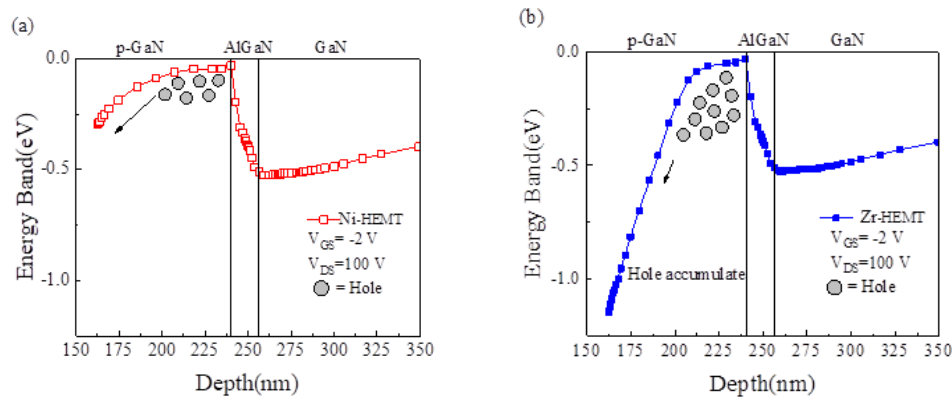


**Figure 4.** Valence band of (a) Ni and (b) Zr contact to p-GaN are simulated by TCAD.

In order to know about the device reliability, Schottky breakdown voltage and off-state breakdown voltage were measured in Figure 5a,b, respectively. In Figure 5a, The Schottky breakdown voltage of Zr-HEMT was improved to 610 V due to the low work function metal contact to p-GaN that formed the high Schottky barrier height. The hole needs more energy to cross the barrier, so the Schottky breakdown can be improved. However, the off-state breakdown also could be improved to 796 V, as shown in Figure 5b. The width of the depletion region is the point in off-state breakdown. The depletion width was widened by high Schottky barrier height due to hole accumulation. Moreover, higher electric field always accompanied high temperature. There is ZrN at the interface of p-GaN and the gate metal, which is a refractory material, it made the device obtain better thermal stability in the gate region.

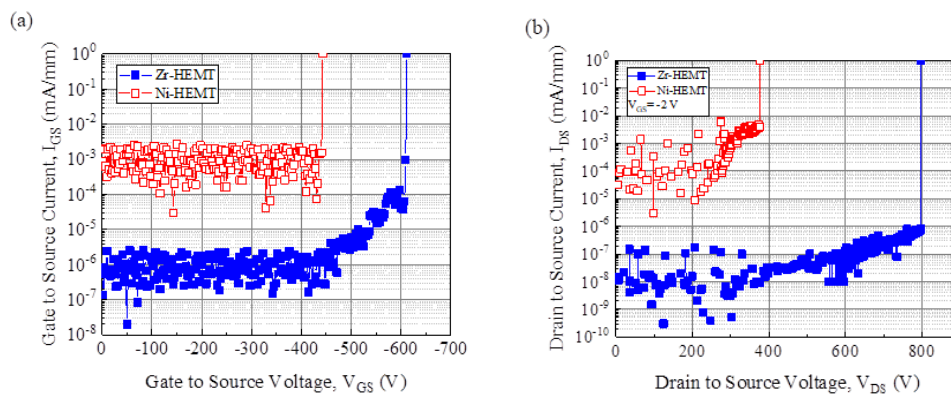


**Figure 5.** (a) Schottky breakdown voltage and (b) off-state breakdown voltage of Zr-HEMT and Ni-HEMT.

For the evaluation of gate lag behavior, we adopted pulse measurement system AM241 [14]. Figure 6a displays the pulsed I–V characteristics of both devices that were switched on from the off state with a  $V_{DSQ}$  of 0 V, the  $V_{GSQ}$  value ranging from 0 to  $-15$  V, a voltage step of  $-5$  V at room temperature, and an on-state gate bias of 5 V. The device was switched on with a pulse width of 2  $\mu$ s and a pulse period of 200  $\mu$ s. However, we also calculated the dynamic  $R_{on}$  ratio in the Figure 6b. Figure 6b shows the shows dynamic on-state  $R_{on}$  behaviors in the conventional and proposed structure

of HEMT after pulsed I–V stress. At the reverse gate bias with  $V_{GSQ} = -5$  to  $-15$  V, the Schottky diode between metal gate and p-GaN was the forward bias. The holes in the p-GaN layer were emitted to the gate metal, so the holes in p-GaN would be reduced. When the  $V_{GS}$  is switched back to the positive bias, this effect may influence the hole injection because the holes in the p-GaN layer cannot be restored immediately [15]. As the result, the Zr-HEMT shows the better dynamic  $R_{on}$  ratio at  $V_{GSQ} = -15$  V, which can be illustrated by the better bonding between p-GaN and Zr and ZrN can also suppress the nitrogen vacancies.

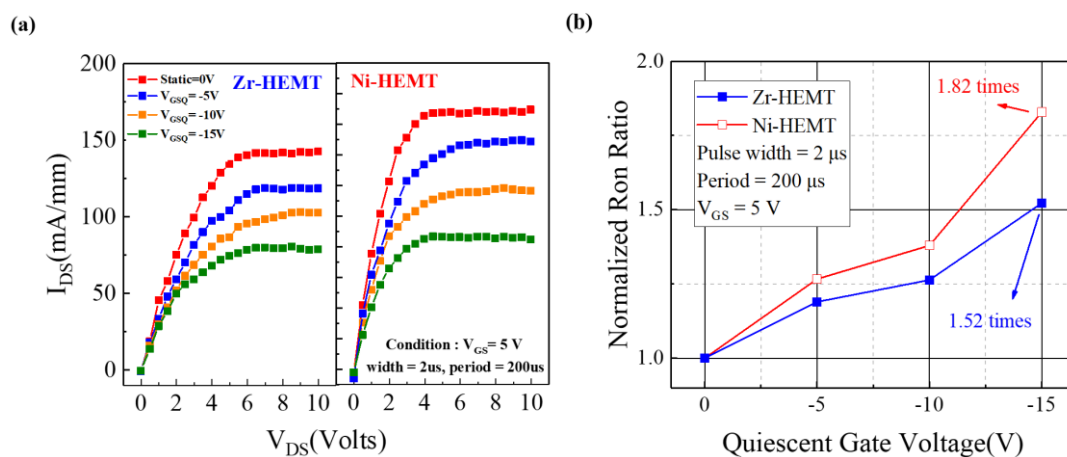


**Figure 6.** (a) Pulse  $I_{DS}$ – $V_{DS}$  characteristics, and (b) dynamic  $R_{on}$  ratio of the Zr-HEMT and Ni-HEMT at different  $V_{GSQ}$ .

#### 4. Conclusions

We investigated the impact of gate metal work function on the leakage current and high breakdown voltage. In addition, ZrN was observed in Zr  $3d_{5/2}$  peaks by XPS analysis. Simulation of the device bandgap by TCAD explained the low work function metal gate Zr contact to p-GaN, which got the higher Schottky barrier height. The higher Schottky barrier height suppressed the hole current and increased the depletion region, which led to device have low leakage current and high breakdown voltage. Therefore, it is important to select the gate metal to control device characteristics. Our discussion above reveals a trade-off between leakage and saturation current in the device with p-GaN/AlGaIn/GaN structure.

**Author Contributions:** C.-H.L., H.-C.C., C.-R.H., K.-J.C. are in charge of experiment and results discussion. K.-J.C. and C.-T.C. provided the epitaxy support and materials. K.-P.H. supported related measurement setup and discussion. All authors have read and agreed to the published version of the manuscript.

**Funding:** This work was supported by the Ministry of Science and Technology (MOST), Taiwan, R.O.C., under Grant MOST 108-2218-E-182-006.

**Conflicts of Interest:** The authors declare no conflict of interest.

#### References

1. Uemoto, Y.; Hikita, M.; Ueno, H.; Matsuo, H.; Ishida, H.; Yanagihara, M.; Ueda, T.; Tanaka, T.; Ueda, D. Gate injection transistor (GIT) normally-off AlGaIn/GaN power transistor using conductivity modulation. *IEEE Trans. Electron Devices* **2007**, *54*, 3393–3399. [[CrossRef](#)]
2. Saito, W.; Takada, Y.; Kuraguchi, M.; Tsuda, K.; Omura, I.; Ogura, T.; Ohashi, H. High breakdown voltage AlGaIn–GaN power-HEMT design and high current density switching behavior. *IEEE Trans. Electron Devices* **2003**, *50*, 2528–2531. [[CrossRef](#)]
3. Cai, Y.; Zhou, Y.; Chen, K.J.; Lau, K.M. High-performance enhancement-mode AlGaIn/GaN HEMTs using fluoride-based plasma treatment. *IEEE Electron Device Lett.* **2005**, *26*, 435–437. [[CrossRef](#)]

4. Tang, Z.; Jiang, Q.; Lu, Y.; Huang, S.; Yang, S.; Tang, X.; Chen, K.J. 600-V normally off SiN<sub>x</sub>/AlGa<sub>n</sub>/Ga<sub>n</sub> MIS-HEMT with large gate swing and low current collapse. *IEEE Electron Device Lett.* **2013**, *34*, 1373–1375. [[CrossRef](#)]
5. Hu, X.; Simin, G.; Yang, J.; Khan, M.A.; Gaska, R.; Shur, M.S. Enhancement mode AlGa<sub>n</sub>/Ga<sub>n</sub> HFET with selectively grown pn junction gate. *Electron. Lett.* **2000**, *36*, 753–754. [[CrossRef](#)]
6. Hilt, O.; Knauer, A.; Brunner, F.; Bahat-Treidel, E.; Würfl, J. Normally-off AlGa<sub>n</sub>/Ga<sub>n</sub> HFET with p-type Ga gate and AlGa<sub>n</sub> buffer. In Proceedings of the 24th International Symposium on Power Semiconductor Devices & ICs, Hiroshima, Japan, 6–10 June 2010; pp. 347–350.
7. Wu, T.-L.; Marcon, D.; You, S.; Posthuma, N.; Bakeroot, B.; Stoffels, S.; Hove, M.V.; Groeseneken, G.; Decoutere, S. Forward bias gate breakdown mechanism in enhancement-mode p-GaN gate AlGa<sub>n</sub>/Ga<sub>n</sub> high-electron mobility transistors. *IEEE Electron Device Lett.* **2015**, *36*, 1001–1003. [[CrossRef](#)]
8. Hwang, I.; Choi, H.; Lee, J.; Choi, H.S.; Kim, J.; Ha, J.; Um, C.-Y.; Hwang, S.-K.; Oh, J.; Kim, J.-Y.; et al. 1.6 kV, 2.9 mohm.cm<sup>2</sup> normally-off p-GaN HEMT device. In Proceedings of the 24th International Symposium on Power Semiconductor Devices & ICs, Bruges, Belgium, 3–7 June 2012; pp. 41–44. [[CrossRef](#)]
9. Saito, W.; Takada, Y.; Kuraguchi, M.; Tsuda, K.; Omura, I. Recessed gate structure approach toward normally off high-voltage AlGa<sub>n</sub>/Ga<sub>n</sub> HEMT for power electronics applications. *IEEE Trans. Electron Devices* **2006**, *53*, 356–362. [[CrossRef](#)]
10. Li, W.; Zhang, Z.; Fu, K.; Yu, G.; Zhang, X.; Sun, S.; Song, L.; Hao, R.; Fan, Y.; Cai, Y.; et al. Design and simulation of a novel E-mode GaN MISHEMT based on a cascode connection for suppression of electric field under gate and improvement of reliability. *J. Semicond.* **2017**, *38*, 074001. [[CrossRef](#)]
11. Roccaforte, F.; Vivona, M.; Nigro, R.L.; Giannazzo, F.; di Franco, S.; Bongiorno, C. Ti/Al-based contacts to p-type SiC and GaN for power device applications. *Phys. Status Solid A* **2017**, *214*, 1600357. [[CrossRef](#)]
12. Hwang, I.; Kim, J.; Choi, H.S.; Choi, H.; Lee, J.; Kim, K.Y.; Park, J.-B.; Lee, J.C.; Ha, J.; Oh, J.; et al. p-GaN Gate HEMTs with Tungsten Gate Metal for High Threshold Voltage and Low Gate Current. *IEEE Electron Device Lett.* **2013**, *34*, 202–204. [[CrossRef](#)]
13. Noda, N.; Tsurumaki, R.; Horio, K. Analysis of lags and current collapse in field-plate AlGa<sub>n</sub>/Ga<sub>n</sub> HEMTs with deep acceptors in a buffer layer. *Phys. Status Solidi C* **2016**, *13*, 341. [[CrossRef](#)]
14. Chiu, H.-C.; Chang, Y.-S.; Li, B.-H.; Wang, H.-C.; Kao, H.-L. High-Performance Normally Off p-GaN Gate HEMT with Composite AlN/Al<sub>0.17</sub>Ga<sub>0.83</sub>N/Al<sub>0.3</sub>Ga<sub>0.7</sub>N Barrier Layers Design. *J. Electron Device Soc.* **2018**, *6*, 201–206. [[CrossRef](#)]
15. Wang, H.; Wei, J.; Xie, R.; Liu, C.; Tang, G.; Chen, K.J. Maximizing the Performance of 650-V p-GaN Gate HEMTs: Dynamic RON Characterization and Circuit Design Considerations. *IEEE Trans. Power Electron.* **2017**, *32*, 5539–5549. [[CrossRef](#)]

